STATIC AND DYNAMIC MAGNETIC END EFFECTS AND CORRECTION MAGNETS FOR THE AGS BOOSTER*

G.T. Danby and J.W. Jackson
AGS Department, Brookhaven National Laboratory
Associated Universities, Inc., Upton, NY 11973 USA

Abstract

The multipurpose Booster under construction has very variable requirements: precision rapid cycling for very high intensity protons and polarized protons, combined with a high vacuum system and a large dynamic range slow cycle for heavy ion acceleration. Magnet ends are shaped to minimize aberrations both internally (2D) and integrally (3D). For the Booster this involves static, magnetization cycle and eddy current fields. The 0.5m long, 16.5 cm bore quadrupoles with shaped ends produce integral 3D values measured at full aperture which are pure quadrupole to ~ 1 x 10^{-4} independent of rise rate. Detailed results are presented. Dipole properties and dipole, quadrupole tracking will be discussed for different cycles.

Quadrupole Results

The desire for maximum understanding and control of high intensity space charge impacted beams in the AGS Booster requires that the magnets be highly accurate and that the lattice then has large tuning control capability. The quadrupoles are designed so that they can be powered either in separate strings or in series with the dipoles. The quadrupoles have been revised with shaped ends configured so that long coil measurements give purely quadrupolar magnetic field integral (3D). Figure 1 shows the quadrupole design. The pole tip diameter = 16.5 cm (6.5 inches) and the magnetic length is ~ 51 cm or only 3 times the bore. Originally, a square end design gave 0.6% of 12-pole aberration due to the ends.

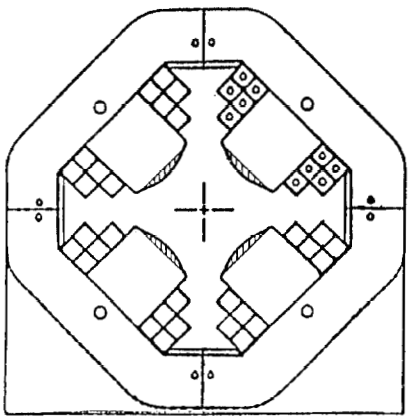

Fig. 1. Booster Quadrupole Cross Section.

A 45° planar end bevel was used on the pole ends. Its amplitude was empirically adjusted based on long coil measurements. Table I shows the results at ρ = 7.62 cm (3 inches). Note that the allowed multipoles are reduced to 1 x 10^{-4} of the quadrupoles at the radius of the vacuum pipe. These multipoles are also within a few parts in 10^4 at the center of the magnet, so end effects are extremely small as seen by the long coil. This magnet had been disassembled and modified several times. The mechanical error terms are larger than desired and are expected to be considerably smaller in production magnets. The nominal tolerances are $\lesssim$ 1 x 10^{-4} with respect to the dipole strength. An additional advantage of shaped ends is that they also reduce dynamical eddy current aberrations. This is because the longitudinal fields which are normal to the thin laminations are reduced. Table II lists in Column I the dynamic multipoles. Magnetization and eddy currents ($\dot{B}$) contribute to the quadrupole (linear) term field integral. This is also true of the dipole and contributes to tune tracking only. The nonlinear aberrations seen by the beam will also be less than 1 x 10^{-4} of the quadrupole's integral.

TABLE I: Booster Quadrupoles
(#2 Prototype with Laminated Shaped Ends)
Integrated Field Measurements at ρ=3 inches
expressed in parts x 10^{-4}

n	a_n	b_n
1	- 14.4†	- 1.33†
2	0	[1 x 10^4]
3	- 12.5	- 2.46
4	- 5.35	- 0.76
5	+ 1.29	- 0.63
6	+ 1.45	[+ 0.20]*
7	+ 0.25	+ 0.02
8	+ 0.31	- 0.63
9	- 0.11	+ 0.17
10	+ 1.04	[+ 0.70]*
11	- 0.05	- 0.06
12	- 0.09	- 0.22
13	+ 0.08	- 0.06
14	+ 0.26	[- 1.41]*

1)* The boxed terms are allowed by mechanical symmetry. Note that the allowed multipoles are <1 x 10^{-4} of the quadrupole integral.
2) All other terms are not allowed by ideal quadrupole symmetry and are due to errors in construction, excitation coil ends, etc.
3)† Dipole terms of ~ 1 x 10^{-3} are arbitrary: magnet construction errors, search coil location and measurement errors all contribute. Corresponds to 0.1 mm centering error.
4) Note that ρ=3 inches is 92% of radius to Fe pole tip.
5) L_Q = 0.517 m.

Column II shows the results, including a model vacuum chamber (VC). In Column III these are scaled to the first VC choice. Note that 12-pole and higher aberrations will contribute $\lesssim$ 1 x 10^{-4} of the integrated quadrupole strength at full beam size. This very linear lens then requires no corrections. (Tune) tracking with the dipoles will be discussed later. The extremely linear lens behavior is as seen by a long coil, not a charged particle. However, for the Booster, these deviations will be very small. The longitudinal field B_z is not seen by

* Work performed under the auspices of the U.S. Department of Energy.

CH2669-0/89/0000-0381$01.00©1989 IEEE

TABLE II: Quadrupole Prototype #2 with Shaped Ends
Eddy Current and Magnetization Measurments†

Multipole	I Bare Quadrupole* (incl. support flanges)		II Quadrupole + Model 316SS Vacuum Chamber		III Results Scaled to Final Inconel Vacuum Chamber	
	ΔB_{mag}	ΔB_{eddy}	ΔB_{mag}	ΔB_{eddy}	ΔB_{mag}	ΔB_{eddy} (Projected)
AC 2**	$+ 22.6\times10^{-4}$	$+ 13.1\times10^{-4}$	$+ 23.9\times10^{-4}$	$+ 47.3\times10^{-4}$	$+ 23\times10^{-4}$	$+24\times10^{-4}$
C 6 (r^5) (12 pole)	$+ 0.25\times10^{-4}$	$+ 2.1\times10^{-4}$	$+ 0.25$	$+ 5.9\times10^{-4}$	$+ 0.25\times10^{-4}$	$+3.0\times10^{-4}$
C 10 (r^9) (20 pole)	$+ 0.44\times10^{-4}$	$- .23\times10^{-4}$	$+ 0.15\times10^{-4}$	$- 0.75\times10^{-4}$	$+ 0.2\times10^{-4}$	-0.4×10^{-4}
C 14 (r^{13}) (28 pole)	$- .12\times10^{-4}$	$- .42\times10^{-4}$	$+ 0.30\times10^{-4}$	$- 1.0\times10^{-4}$	$+ 0.2\times10^{-4}$	-0.5×10^{-4}

1) †Integral (LC) measurements for $\dot{B}$ = 6T/sec in quadrupole. (This is equivalent to 9T/sec in dipole.)
2) "Bare" measurements are at R=3.125": Vacuum chamber measurements scaled to R=3.125".
3) ΔB_{mag} and ΔB_{eddy} are expressed at (dipole=0.25T), 50% of final proton momentum which is approximately at maximum B/B. All amplitudes are parts in 10^{-4} of gradient integral of quadrupole.
4) Inconel has a conductivity 0.57 x 316 stainless steel. It is also stronger, so thinner wall is possible. Column III eddy currents assume 50% conductivity compared to model.
5) We have no corrections for 12-pole or higher.
6) Note that if a particle filled the aperture at injection, r=3, by B=0.25T, phase space shrinkage gives a radius of R=2.4". This would reduce 12-pole (C6) to 0.35 times listed number.
7) In Summary: higher multipoles due to magnetization or eddy currents (including vacuum chamber!) contribute $\lesssim 1\times10^{-4}$ to the quadrupole. (Furthermore, the quadrupole is ~ 8 times weaker than the dipole.)
* The "bare" quadrupole includes small contributions from stainless steel flanges at each end. These are designed to automatically center the vacuum chamber and PUE accurately.
** The CHANGE in the quadrupole term ΔC2 due to magnetization and eddy currents is large. Thus, the gradient integral strength will vary with $\dot{B}$. The is expected and affects the tune. It can be corrected by programming or servoing the power supplies. Note the above ΔC2 is for $\dot{B}/B$=9T/sec/0.25T, which is large.

the long coils. Thus the quite small radial components of velocity will interact with B_z to give a weak deflection out of plane. In the transverse planes the variation of $\sqrt{\beta}$ over the short quadrupoles is very small, and furthermore is the same at both ends. This then closely mimics the long coil.

Dipole Results

The dipole magnets contain laminated wedges producing a 10^0 bend with normal beam incidence on each end. The gap is 8.26 cm (3.25 inches) and the magnetic length is nominally 2.40 m, or 30 times the gap. Shaped ends have been studied but for simplicity, square ends are being used. Heavy Ion operation requires cycling to an integral strength of 1.274T x 2.40 m. Figure 2 shows results for a long integrating curved coil measurement of a magnet cycle slightly higher.

Curve 1 gives the measured variation with radius. Curve 4 is obtained by left-right differences This shows a gradient which is linear to beyond R=2 inches. Note that this gradient is predominantly due to the 10^0 ends of the magnet, slightly modified by high field saturation. Curve 2 shows the left-right averages. Curve 3 shows that a sextupole correction, which is within the capability of the lattice sextupoles, can correct to beyond R=2 inches. Note that R=±2 inches is much more aperture than required at top energy. The large sextupole is only present at the highest fields. It is due to saturation and is predominantly an end effect. Figure 3 shows that magnetization and eddy currents contribute very little to the heavy ion cycle field shape.

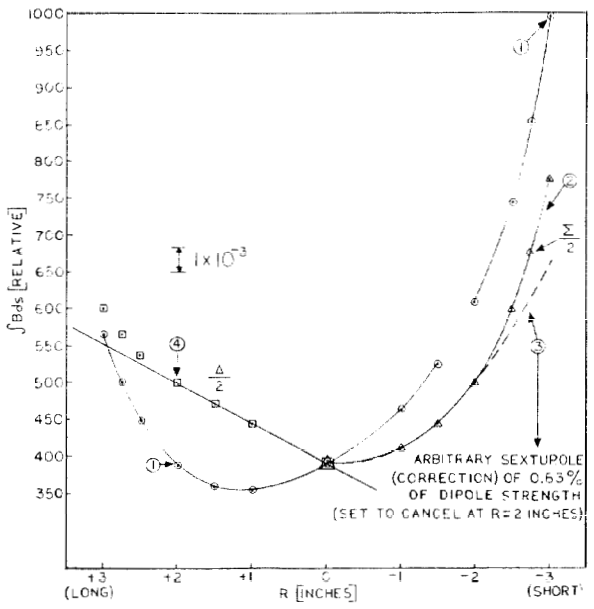

Fig. 2. Integrated Dipole Magnetic Field vs Radius.

Thus with tune control and sextupoles (Fig. 2), a large linear aperture is available at all fields.

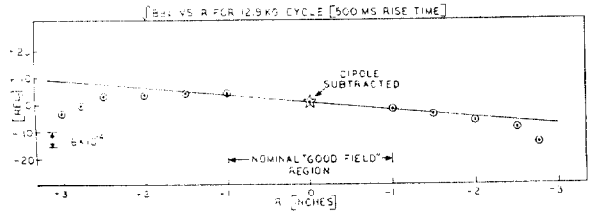

Fig. 3. Magnetization and Eddy Current Effect for Dipole.

Long coil results for the proton cycle are shown in Fig. 4. Curve 1 shows the radial variations of magnetization and eddy currents. Cycle b (1/10 rise rate) shows a very small, completely constant dipolar term. Cycle a (8T/sec) shows a small gradient (slope) which will require very small adjustment in tune, plus sextupole-like nonlinearity of $\sim 2 \times 10^{-4}$ parts at $\rho = 3$ inches.

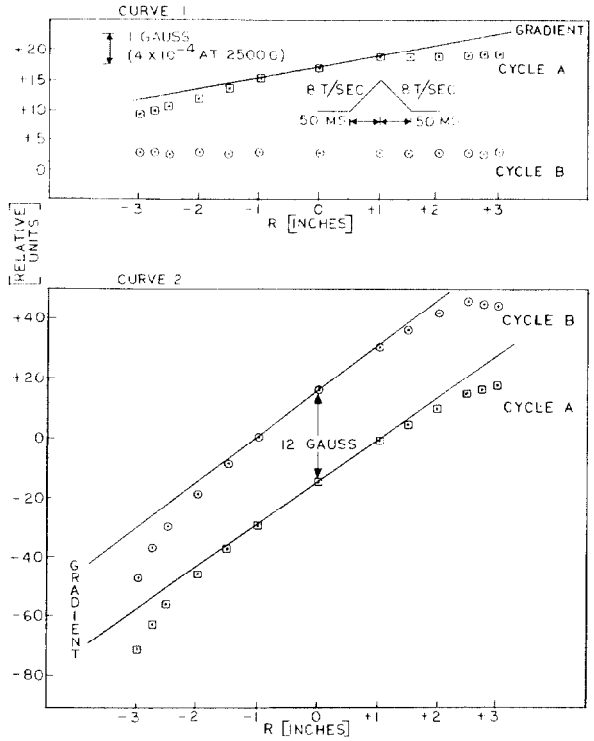

Fig. 4. Magnetization, Eddy Currents and Field Integral for Two Cycles.

Curve 2 shows the actual field integral from 1.6 kG to 5.6 kG. The gradient slope is due to the 10° ends. The sextupole-like effects are due to magnet ends: inside the magnet is very flat and dipolar. Note the displacement between the fast and slow cycles. The dipole field is shorter by 0.7 cm for 8T/sec rise rate. End effects were measured using a 61 cm long coil inserted into an end of the magnet. The standard square end was compared to a shaped end employing an approximation of two plane surfaces.

Figure 5 shows the radial non-linearity with fast and slow cycles. The shaped end is better by about 50%. Figure 6 shows the dipolar part, measured at R=0 as a function of dB/dt. The larger magnetization (slow cycles) of the square end is due to the material choice; i.e., M45 versus M36 steel.

The eddy current dipole change is considerably larger than for the shaped end. This, however, is optically a tracking (tune) question.

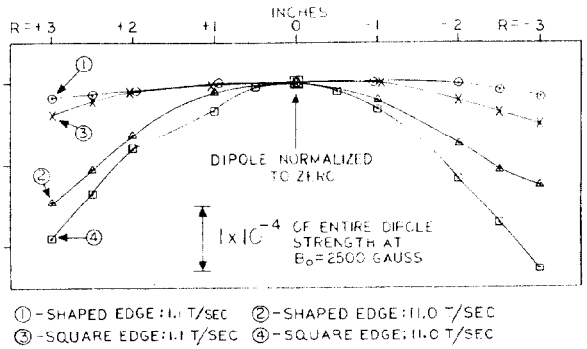

Fig. 5. Radial Nonlinearity, Magnetization Plus Eddy Current

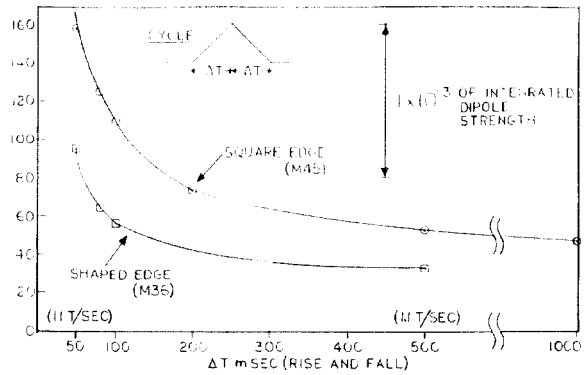

Fig. 6. Dipole End Effects, Magnetization Plus Eddy Current

The dipole prototype measurements at R=0 with the long curved coil showed for the proton pulsed cycle a contribution to the field due to magnetization of 5.6 gauss. Eddy currents increase this offset by 3.6 gauss for dB/dt = 11T/sec. These results include end effects: measurements inside the magnet gave a magnetization of 4 gauss and no significant eddy currents. Thus at dB/dt = 8T/sec and B_o=0.25T, end eddy currents will contribute 11 x 10^{-4} and magnetization 22 x 10^{-4}. Measurements with the long curved coil at R=0 of the prototype showed the dipole field component saturates by 10% at maximum heavy ion excitation. This is predominantly not an end effect. It can be predicted by the computer code, assuming the steel packing factor. The saturation of the dipole and of the quadrupole were designed on the computer to be the same (in 2D) for the same excitation currents. Preliminary tracking measurements have been made using the final quadrupole prototype and the dipole. These indicate that if operated in series, saturation, magnetization and eddy currents will track to within 1%. Auxiliary coil excitation of the quadrupoles can control the final ~1% for precise tune control. Furthermore this conclusion appears to hold even if vacuum chamber (VC) fields are included. Table II showed that 12-pole, etc., aberrations are very small, even with quadrupole VC included. In a companion paper it is demonstrated that self-correction coils can automatically suppress by transformer action the nonlinearity in the dipole VC. The fundamental components, quadrupole and dipole VC eddy currents will also contribute to the tracking auxiliary current requirements.